IFAC Journal of Systems and Control 31 (2025) 100294

Contents lists available at ScienceDirect

IFAC Journal of Systems and Control

journal homepage: www.elsevier.com/locate/ifacsc

Full length article

CHoKI-based MPC for blood glucose regulation in Artificial Pancreas

Beatrice Sonzogni [a,*], José María Manzano [b], Marco Polver [a], Fabio Previdi [a], Antonio Ferramosca [a]

[a] Department of Management, Information and Production Engineering, University of Bergamo, 24044 Dalmine, Bergamo, Italy
[b] Department of Engineering, Universidad Loyola Andalucía, 41704 Dos Hermanas, Seville, Spain

ARTICLE INFO

Article history:
Received 8 November 2023
Received in revised form 26 November 2024
Accepted 22 December 2024
Available online 1 January 2025

Keywords:
Artificial Pancreas
MPC
Learning-based control

ABSTRACT

This work presents a Model Predictive Control (MPC) for the artificial pancreas, which is able to autonomously manage basal insulin injections in type 1 diabetic patients. Specifically, the MPC goal is to maintain the patients' blood glucose level inside the safe range of 70-180 mg/dL, acting on the insulin amount and respecting all the imposed constraints, taking into consideration also the Insulin On Board (IOB), to avoid excess of insulin infusion. MPC uses a model to make predictions of the system behavior. In this work, due to the complexity of the diabetes disease that complicates the identification of a general physiological model, a data-driven learning method is employed instead. The Componentwise Hölder Kinky Inference (CHoKI) method is adopted, to have a customized controller for each patient. For the data collection phase and also to test the proposed controller, the virtual patients of the FDA-accepted UVA/Padova simulator are exploited. The MPC is also tested on simulations with variability of the insulin sensitivity and with physical activity sessions. The final results are satisfying since the proposed controller is conservative and reduces the time in hypoglycemia (which is more dangerous) if compared to the outcomes obtained without the IOB constraints.

1. Introduction

Diabetes is a common chronic metabolic disorder characterized by the body's inability to correctly balance the Blood Glucose (BG) level, due to the absence or not enough insulin production by the pancreas. In particular, Type 1 Diabetes (T1D) is characterized by the autoimmune destruction of the insulin-producing beta cells. This drives the patient into a state of hyperglycemia, so when the BG level is above 180 mg/dL, which has long-term complications, such as cardiovascular disease, neuropathies or kidney damage. Thus, T1D patients require daily insulin injections to maintain the BG level inside the euglycemic range (i.e. between 70 and 180 mg/dL). Below this threshold, the patient is in a state of hypoglycemia, which is dangerous in the short-term since can even lead to the diabetic coma (Katsarou et al., 2017). In order to ease patients' and caregivers' life, the therapy is trying to get more and more automatized, miming the functioning of a healthy pancreas. Specifically, the Artificial Pancreas (AP) implements such a treatment in a closed loop. It is a system made of three components: the sensor that measures the glucose at the interstitial level every few minutes (Continuous Glucose Monitoring, CGM), and the control algorithm that computes the insulin amounts that are then injected into the subcutaneous tissue through the pump. The APs currently on the market are hybrid closed loop systems, since the administration of the basal insulin (which is the small, continuous and constant amount injected to manage the BG in fasting periods) is automatic, while for postprandial boluses (i.e. bigger amount injected at meal times to face the BG increase due to carbohydrate ingestion or when the BG level is unexpectedly too high) it still requires the manual intervention of the patients (Moon, Jung, & Park, 2021).

Model Predictive Control (MPC), due to its predictive capability and the possibility to add constraints to the problem, is one of the most widely used control algorithms for the AP. MPC is a control strategy that uses a dynamic model to forecast the future behavior of a system. Based on this prediction, it calculates the best sequence of control actions at every sampling time, by solving a finite horizon optimal control problem. Then, only the first value of the control action sequence is applied to the system and the process is repeated at each sampling time, in a receding horizon fashion (Rawlings, Blake, & Mayne, 2009). Over the last few years, the use of MPC as a control algorithm for AP has been extensively studied and tested (Abuin, Rivadeneira, Ferramosca, & González, 2020; Cairoli, Fenu, Pellegrino, & Salvato, 2020; Del Favero, Toffanin, Magni, & Cobelli, 2019; Gondhalekar, Dassau, & Doyle III, 2016; González, Rivadeneira, Ferramosca, Magdelaine, & Moog, 2017, 2020; Hajizadeh, Rashid, & Cinar, 2019; Hovorka et al., 2004; Shi, Dassau, & Doyle, 2018; Soru et al., 2012; Toffanin et al., 2013), thanks to its capability to anticipate unwanted fluctuations

* Corresponding author.
E-mail address: beatrice.sonzogni@unibg.it (B. Sonzogni).

https://doi.org/10.1016/j.ifacsc.2024.100294

in glycemic levels and to calculate the amount of insulin to be injected, taking into account all the constraints.

T1D is a disease that varies both among and within patients and this is due to differences in the blood glucose response to meals or insulin, which can also vary according to daily state. Identifying a general model to describe the insulin-glucose system is therefore difficult. This work aims to use data-driven approaches, that is, to use the current and past data of a patient to obtain the future BG, and then to be able to calculate the correct amount of basal insulin to be delivered. This facilitates and improves T1D management by providing a customized MPC algorithm for the AP. Recently, different types of learning-based MPCs have been proposed in the literature (Hewing, Wabersich, Menner, & Zeilinger, 2020), which are based on different learning methods. Specifically, we use the Componentwise Hölder Kinky Inference (CHoKI) method, a nonparametric learning technique that favors the design of robust MPCs that are stable by design (Manzano, Muñoz de la Peña, Calliess, & Limon, 2021).

In this case, starting from the work proposed in Sonzogni, Manzano, Polver, Previdi, and Ferramosca (2023), in the MPC optimization problem is considered also a dynamic safety constraint on the maximum basal insulin value, which is based on the Insulin On Board (IOB). To take into account the insulin amount of the boluses that is still active in the patient, when computing the quantity of the basal corrections, to reduce the risk of hypoglycemic events.

The virtual patients of the UVA/Padova simulator (The Epsilon Group, 2016) are exploited to collect the data needed to learn the system behavior and also to test the proposed control algorithms. This is a simulator accepted by the Food and Drug Administration (FDA) as a substitute for pre-clinical studies and it contains populations of virtual subjects; in particular, we have used the adults with T1D.

The same proposed CHoKI-based MPC has been also tested on patients whose insulin sensitivity varies intra-subjects throughout the day. Moreover, other simulations are performed to assess the controller's ability to deal with physical activity sessions.

The rest of this work is structured as follows: Section 2 presents the CHoKI learning method and the version tailored to the T1D patient case. Section 3 analyses the proposed model predictive control problem. The implementation of the designed controller in the UVA/Padova simulator is presented in Section 4, and Section 5 concludes the paper.

Notation:

A set of integers $[a, b]$ is denoted $\mathbb{I}_a^b$, $\mathbb{R}^n$ is the set of real vectors of dimension n and $\mathbb{R}^{n\times m}$ is the set of real matrices of dimension $n\times m$. Given $v, w \in \mathbb{R}^{n_v}$, the notation (v, w) implies $[v^T, w^T]^T$ and $v \leq w$ implies that the inequality holds for every component. $\|v\|$ stands for the Euclidean norm of v and $|v| = \{w : w_i = |v_i|, \forall i\}$. Given two sets A, B, $A \ominus B$ denotes the Pontryagin difference. Their Cartesian product is denoted $A \times B = \{(x, y)|x \in A, y \in B\}$. The positive box $\mathbb{B}(v) \subset \mathbb{R}^{n_v}$ of radius v is defined as $\mathbb{B}(v) = \{y : 0 \leq y \leq v\}$ and the ball $\mathcal{B}(v) \subseteq \mathbb{R}^{n_v}$ of radius v is defined as $\mathcal{B}(v) = \{y : |y| \leq v\}$. An n, m-dimensional matrix of ones is denoted $\mathbb{1}_{n\times m}$. The ith row of a matrix M is denoted M_i.

2. Problem statement

The analyzed problem is based on the CHoKI formulation proposed in Sonzogni et al. (2023), which is briefly reported in the following.

The system is a sampled continuous-time one, described by an a priori unknown discrete-time model, whose measured output is $y(k) \in \mathbb{R}^{n_y}$ and whose input is $u(k) \in \mathbb{R}^{n_u}$. In this case, there is one output ($n_y = 1$) which is the glucose level, in mg/dL, and there are two inputs ($n_u = 2$), which are the meal (u_1, the disturbance) in g of carbohydrates and the insulin (u_2, the manipulated variable) in pmol. A sampling time of 5 min is considered.

The measured output can be modeled as a nonlinear autoregressive exogenous (NARX) model, with the following state-space representation:

$$y(k+1) = f\big(x(k), u_1(k), u_2(k)\big) + e(k),$$

where $e(k) \in \mathbb{R}^{n_y}$ is process noise and the regression state $x \in \mathbb{R}^{n_x}$ is

$$x(k) = \Big(y(k), \dots, y(k-n_a), u_1(k-1), \dots, u_1(k-n_b), \\ u_2(k-1), \dots, u_2(k-n_c) \Big), \tag{1}$$

where $n_a \in \mathbb{N}_0$ is the memory horizon for the glucose values, $n_b \in \mathbb{N}_0$ for the meals and $n_c \in \mathbb{N}_0$ for the basal insulin injections. The arguments of f are then aggregated into $w = (x, u_1, u_2) \in \mathbb{R}^{n_w}$ so that it is possible to build a data set of $N_{\mathcal{D}}$ observations, denoted $\mathcal{D} = \{(y_{k+1}, w_k)\}$, for $k = 1, \dots, N_{\mathcal{D}} - 1$.

2.1. Componentwise Hölder Kinky Inference (CHoKI)

The purpose of this subsection is to be an introduction to the choice of learning method. Kinky Inference (KI) (Manzano, Limon, Muñoz de la Peña, & Calliess, 2020) is a class of learning approaches that includes Lipschitz interpolation, which is a technique based on Lipschitz continuity of the ground truth function. There exists an extension of the Lipschitz continuity, named Hölder continuity, defined as follows:

Definition 1 (*Hölder Continuity*)**.** *A function $f : \mathcal{W} \to \mathcal{Y}$ is Hölder continuous if there exist two real constants $L \geq 0$ and $0 < p \leq 1$ such that for all $w_1, w_2 \in \mathcal{W}$,*

$$\|f(w_1) - f(w_2)\| \leq L\|w_1 - w_2\|^p, \tag{2}$$

where L represents the smallest Lipschitz constant and p is called the Hölder exponent, $\mathcal{W} \subseteq \mathbb{R}^{n_w}$ is the input space and $\mathcal{Y} \subseteq \mathbb{R}^{n_y}$ is the output space.

In the case of $p = 1$, it means to have Lipschitz continuity (Manzano et al., 2021).

To catch different variations of the output according to the changes of each component of the input regressor, the Componentwise Hölder Kinky Inference (CHoKI) (Manzano et al., 2021) can be implemented. This method is based on the componentwise Hölder continuity, which considers matrices $\mathcal{L}$ and $\mathcal{P}$, instead of the Hölder constant L and exponent p. This is useful in cases where a function may have sudden variations along one dimension of the input, while changing smoothly along other input dimensions.

Definition 2 (*Componentwise Hölder Continuity*)**.** Given the matrices $\mathcal{L}$ and $\mathcal{P} \in \mathbb{R}^{n_y \times n_w}$, a function $f : \mathcal{W} \to \mathcal{Y}$ is componentwise $\mathcal{L}$-$\mathcal{P}$-Hölder continuous if $\forall w_1, w_2 \in \mathcal{W}$ and $\forall i \in \mathbb{I}_1^{n_y}$

$$|f(w_1) - f(w_2)| \leq \mathfrak{d}_{\mathcal{L}}^{\mathcal{P}}(|w_1 - w_2|) \tag{3}$$

where

$$\mathfrak{d}_{\mathcal{L}}^{\mathcal{P}}(w) := \Big(a : a_i = \sum_{j=1}^{n_w} \mathcal{L}_{i,j} w_j^{\mathcal{P}_{i,j}}, \forall i \in \mathbb{I}_1^{n_y}\Big). \tag{4}$$

Then, assuming that f is Hölder continuous and given a data set $\mathcal{D}$ of inputs/outputs observations, the CHoKI predictor for a

query $q \in \mathbb{R}^{n_w}$ is:

$$\hat{f}(q;\Theta,\mathcal{D}) = \frac{1}{2}\min_{i=1,\dots,N_{\mathcal{D}}}\left(\tilde{y}_i + \vartheta_{\mathcal{L}}^{\mathcal{P}}\left(|q-w_i|\right)\right) + \frac{1}{2}\max_{i=1,\dots,N_{\mathcal{D}}}\left(\tilde{y}_i - \vartheta_{\mathcal{L}}^{\mathcal{P}}\left(|q-w_i|\right)\right), \tag{5}$$

where $\Theta = \{\mathcal{L},\mathcal{P}\}$ and $\hat{f}$ is still componentwise $\mathcal{L}$-$\mathcal{P}$-Hölder continuous.

According to (5) it is possible to predict a new output $\hat{y}(k+1) = \hat{f}\left(w(k);\Theta,\mathcal{D}\right)$. Then, the prediction model can be formulated in state-space as follows:

$$\begin{aligned}\hat{x}(k+1) &= \hat{F}\left(x(k),u_1(k),u_2(k)\right)\\ \hat{y}(k) &= M\hat{x}(k)\end{aligned} \tag{6}$$

where $\hat{F}\left(x(k),u_1(k),u_2(k)\right) = \left(\hat{f}(x(k),u_1(k),u_2(k)),y(k),\dots,y(k-n_a+1),u_1(k),\dots,u_1(k-n_b+1),u_2(k),\dots,u_2(k-n_c+1)\right)$ and $M = [I_{n_y},0,\dots,0]$.

If the matrices $\mathcal{L}$ and $\mathcal{P}$ are unknown a priori, they must be estimated. To do that, an optimization problem is solved offline, splitting the data set $\mathcal{D}$ into two disjoint data sets: $\mathcal{D}_{\text{train}}$ for the estimation and $\mathcal{D}_{\text{test}}$ for the validation. The optimization problem is:

$$\Theta = \arg\min_{\Theta} g(\Theta,\mathcal{D}_{\text{train}},\mathcal{D}_{\text{test}}) \tag{7a}$$

$$\text{s.t. } |\tilde{y}_i - \tilde{y}_j| \le \vartheta_{\mathcal{L}}^{\mathcal{P}}(|w_i - w_j|), \quad \forall w_i, w_j \in \mathcal{W}_{\mathcal{D}},\ w_i \neq w_j \tag{7b}$$

$$0 < \mathcal{P}_{ij} \le 1,\ \mathcal{L}_{ij} > 0, \quad i \in \mathbb{I}_1^{n_y},\ j \in \mathbb{I}_1^{n_w}, \tag{7c}$$

where $\mathcal{W}_{\mathcal{D}}$ represents the input data points in $\mathcal{D}$. The cost function $g(\Theta,\mathcal{D}_{\text{train}},\mathcal{D}_{\text{test}})$ to be minimized is:

$$g(\Theta,\mathcal{D}_{\text{train}},\mathcal{D}_{\text{test}}) = \frac{1}{N_{\mathcal{D}_{\text{test}}}}\sum_{i=1}^{N_{\mathcal{D}_{\text{test}}}} \|\hat{f}(w_i;\Theta,\mathcal{D}_{\text{train}}) - \tilde{y}_i\|^2, \tag{8}$$

being $\hat{f}(w_i;\Theta,\mathcal{D}_{\text{train}})$ the predictions made with the CHoKI in (5) (computed with the data in $\mathcal{D}_{\text{train}}$), which are compared to $\tilde{y}_i$, that are the measured values of the noisy data set $\mathcal{D}_{\text{test}}$.

2.2. CHoKI implementation for T1D patient

In this subsection, the CHoKI method explained in Section 2.1 is designed to learn the dynamics of the T1D patient.

To this aim, to implement the CHoKI strategy, the first step is the data collection. This is a fundamental phase since the quality of the generated data set will affect the performance of the CHoKI predictor and thus the functioning of the controller. This is done by employing the virtual T1D adult patients of the UVA/Padova simulator. For each of them, several simulations were made, varying the initial glycemic condition, the basal insulin quantity (from 0 to 500 pmol) and the carbohydrates of the meals (with the post-prandial boluses, given 20 min after the meal time). All these simulations were set to obtain an appropriate distribution of the points in the space, looking at the input–output representation. The simulator allows the inclusion of some noises on the sensor and on the pump, to perform more realistic simulations. Specifically, the available virtual typical commercial CGM was selected as a sensor, with auto-regressive noise with inverse Johnson transform distribution. The noise on the virtual pump is normally distributed with a mean of 0 pmol and a standard deviation of 0.1. Also, an error with a normal distribution with a standard deviation equal to 30% of the meal amount is added to the carbohydrate estimation.

Only the relationship between BG, meals and basal insulin is considered, as the aim of the proposed controller is to manage basal insulin injections automatically, while meal boluses are delivered manually (assuming they are a function of meals). The CHoKI requires the data to be in the right NARX shape, thus the model orders n_a, n_b and n_c have to be identified and this is done through a cross-validation procedure.

In particular, many combinations of model orders were tested. The Root Mean Squared Error (RMSE) among the 1-step ahead predictions and the actual values were measured on an unused 21-day data set. The selected orders were chosen based on the lowest RMSEs, but a trade-off with model complexity was also considered to avoid the risk of overfitting. The resultant orders are $n_a = 5$, $n_b = 9$ and $n_c = 3$, being each sampling time 5 min long.

To obtain the predictions employing (5), the hyperparameters $\Theta = \{\mathcal{L},\mathcal{P}\}$ must be estimated according to (7). We assumed to have $\mathcal{P} = \mathbb{1}_{n_y \times n_w}$ and thus the optimization problem is solved to obtain just the values of the matrix $\mathcal{L}$. In this case, only three values are estimated: $L_a \in \mathbb{R}$ for the glucose part, $L_b \in \mathbb{R}$ for the meals and $L_c \in \mathbb{R}$ for the insulin. Therefore, $\mathcal{L}$ contains those three values repeated to reach the right dimension (i.e. the regressor length n_w), thus $\mathcal{L} = [L_a\mathbb{1}_{n_a}; L_b\mathbb{1}_{n_b}; L_c\mathbb{1}_{n_c}]$.

Some a priori knowledge was utilized in order to set the constraints of the optimization problem: as the $\mathcal{L}$ initial value the Lipschitz constant L was exploited, which is obtained from the LACKI (Lazily Adapted Constant Kinky Inference) method (Manzano et al., 2020), based on the Hölder continuity property. The upper and lower bounds for L_a, L_b and L_c were set as [10;10;10] and [0;0.9;0.09], respectively, thanks to previous analyses.

The `fmincon` MATLAB function was implemented to solve the optimization problem (7). For each patient, once the $\mathcal{L}$ is found, the model is validated on a new data set, to verify its ability to predict future BG values, comparing them with the real outputs. The outcomes of the validation are reported in Table 1, where the RMSE and the GoF (goodness of fitting) are shown, comparing the predictions and the real data of the validation data set (4 days). Specifically, $RMSE = \sqrt{\frac{\sum_{i=1}^{N_{\text{val}}}(y_i-\hat{y}_i)^2}{N_{\text{val}}}}$ and $GoF = 100\left(1 - \frac{\|y_i-\hat{y}_i\|}{\|y_i-\bar{y}_i\|}\right)$, where N_{val} is the number of data in the validation dataset, y_i are the real values, $\hat{y}_i$ are the predictions of the next BG sample and $\bar{y}_i$ is the mean value. For each subject, the resulting $\mathcal{L}$, the u_{ref} and the L are reported in Table 2.

Further analysis was also carried out, starting with a fixed regressor and varying the input values, to ensure that the CHoKI strategy had correctly learned the effect of each input on the output. The fixed regressor has BG set to 120 mg/dL, no meals and constant basal insulin equal to the reference value u_{ref} of each patient, obtained from the standard therapy provided by the simulator. As an example, the results obtained from subject Adult 9 are displayed in Fig. 1: it can be seen how the glucose trend (blue lines) decreases when the amount of the basal insulin injections increases and it rises when there is carbohydrate ingestion. This holds for all the considered virtual patients.

3. CHoKI-based robust MPC

The control objective is to drive and maintain the BG level inside the euglycemic zone, which is given by 70 and 180 mg/dL, satisfying all the inputs and output constraints. The basal insulin amount $u_2(k)$ must be inside the range $\mathcal{U} = \{u : 0 \le u \le 500\text{ pmol}\}$, $\forall k$. It is the control action, whose values are calculated so that the BG level $y(k)$ remains in the set $\mathcal{Y} = \{y : 55 \le y \le 300\text{ mg/dL}\}$, $\forall k$, not to arrive to extreme hyper- or hypoglycemic conditions. An additional constraint is set on the maximum value of the basal insulin, according to the IOB estimation.

In this case, the open-loop predictions of the MPC control problem are computed with the CHoKI predictor (5), assuming that a physiological model for T1D patients is not available. To ensure the robustness of the MPC to possible model-system

Table 1
RMSE and GoF (validation).

Adult	#1	#2	#3	#4	#5	#6	#7	#8	#9	#10	mean value
RMSE	9.28	7.59	7.38	5.98	9.21	7.65	15.21	5.84	9.32	7.17	8.46
GoF	78.59	77.65	72.97	84.67	74.92	82.23	72.23	86.14	82.41	77.61	78.94

Table 2
MPC settings.

Adult	u_{ref} [pmol]	$N_{\mathcal{D}}$	L (LACKI)	$[L_a; L_b; L_c]$ (CHoKI)	μ (90%) [mg/dL]	N_c	ϵ	Q
#1	122.38	4775	3.46	[0.74; 5.46; 0.29]	14.83	2	10	1
#2	134.89	4950	3.28	[4.89; 3.96; 0.09]	10.19	2	20	1
#3	149.97	4990	3.08	[0.71; 5.45; 0.09]	9.29	3	10	1
#4	95.07	4768	3.21	[0.87; 9.94; 0.13]	8.19	3	10	1
#5	91.83	4156	6.56	[0.84; 5.52; 0.44]	13.91	2	5	1
#6	190.22	5339	3.41	[4.72; 3.52; 0.09]	11.27	1	1	1
#7	124.923	4803	4.09	[9.80; 0.9; 1.39]	11.89	1	10	1000
#8	105.83	4703	2.58	[1.08; 5.84; 0.09]	7.8	3	1	100
#9	94.59	3976	3.72	[1.13; 4.09; 0.09]	11.63	2	1	100
#10	124.86	4966	3.29	[3; 2; 0.09]	10.1	1	20	1

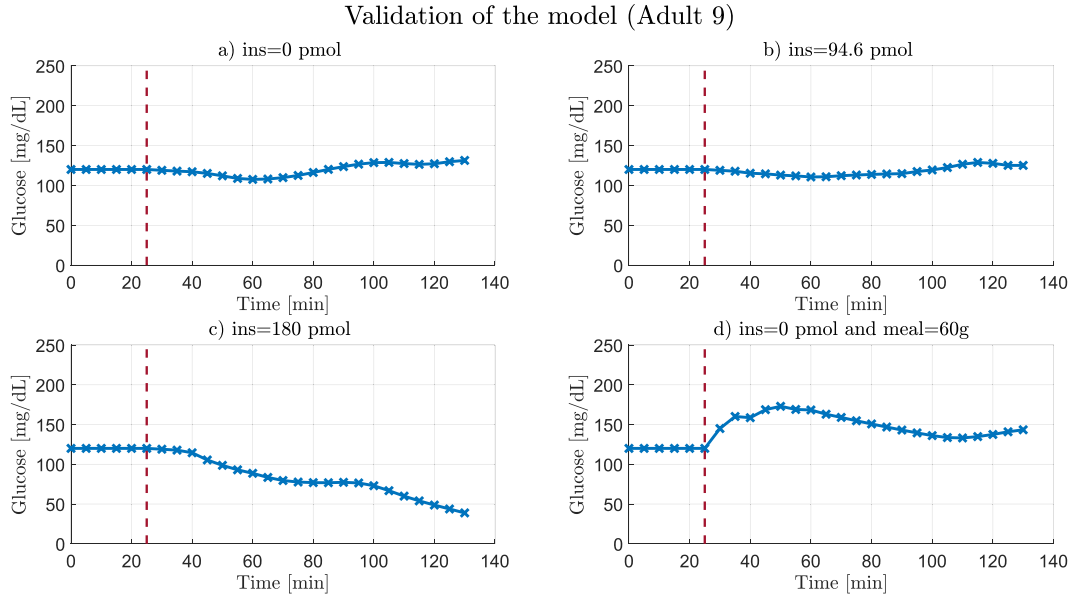

Fig. 1. In each graph, the vertical dashed red line marks the end of the fixed regressor, when the inputs displayed in the titles are applied. The blue line is the glucose trend. In a) the glucose increases a bit, due to the absence of basal insulin. In b) the glucose remains stable since the insulin amount is the reference value and equal to the regressor values. In c) the glucose decreases due to the basal amount of 180 pmol. In d) the glucose increases due to the presence of the meal and no basal insulin.

mismatches, the output constraints are tightened at each step according to an error that represents the uncertainty of the predictions based on the data. The system in closed loop is shown to be Input-to-State Stable (ISS) (Manzano et al., 2021, Theorem 3) with the proposed controller.

The set of restricted output constraints is given by

$$\mathcal{Y}_j = \mathcal{Y}_{j-1} \ominus \mathcal{R}_j, \tag{9}$$

along the prediction horizon, $j = 1, \dots, N$. $\mathcal{R}_j$ are the reachability sets that account for the possible errors in the nominal predictions and $\mathcal{Y}_0 = \mathcal{Y}$. To compute $\mathcal{R}_j$, the starting point is to consider a sequence of future inputs $u(k+1)$ and $c_1 \in \mathbb{R}^{n_y}$, such that

$$|y(k+1) - \hat{y}(1|k)| \leq c_1. \tag{10}$$

The difference between a prediction made at time step $k+j$ based on the measurement at step k, and the prediction made at step k based on the measurement at step $k+1$, for a given sequence of control inputs, is bounded by the sets

$$|\hat{y}(j|k) - \hat{y}(j-1|k+1)| \in \mathcal{M}_j \subseteq \mathbb{R}^{n_y}, \tag{11a}$$

$$|\hat{w}(j|k) - \hat{w}(j-1|k+1)| \in \mathcal{G}_j \subseteq \mathbb{R}^{n_w}. \tag{11b}$$

The sets $\mathcal{M}$ and $\mathcal{G}$ can be calculated from the equations

$$\mathcal{M}_j = \mathbb{B}\big(\mathfrak{d}_{\mathcal{L}}^{\mathcal{P}}(\mathcal{G}_{j-1})\big), \tag{12a}$$

$$\mathcal{G}_j = \mathcal{M}_j \times \cdots \times \mathcal{M}_{\sigma(j)} \times \{0\} \times \cdots \times \{0\}, \tag{12b}$$

with $\sigma(j) = \max(1, j - n_a)$ and $\mathcal{M}_1 = \mathbb{B}(c_1)$. The set $\mathcal{R}_j$ is defined as $\mathcal{R}_j = \{y : |y| \in \mathcal{M}_j\}$ for all $j \in \mathbb{I}_1^N$.

In Manzano et al. (2021) is also shown that $c_j \in \mathbb{R}^{n_y}$ and $d_j \in \mathbb{R}^{n_w}$ are such that $\mathcal{M}_j = \mathbb{B}(c_j)$ and $\mathcal{G}_j = \mathbb{B}(d_j)$. Then, the sets $\mathcal{M}_j$ and $\mathcal{G}_j$ can be computed using the recursion

$$c_j = \mathfrak{d}_{\mathcal{L}}^{\mathcal{P}}(d_{j-1}), \tag{13a}$$

$$d_j = (c_j, \dots, c_{\sigma(j)}, 0, \dots, 0), \tag{13b}$$

with $c_1 = \mu$ (where μ is the maximum absolute error obtained in the validation phase) and then, $\mathcal{R}_j = \mathcal{B}(c_j)$.

In our specific control problem, an *a posteriori* analysis showed that extreme deviations from nominal predictions are highly unlikely. Then, the value representing the 90$^{\text{th}}$ percentile of the probability distribution is used as μ instead of the maximum error (see Table 2).

Remark 1. To deal with the infeasibility of possible solutions outside the 90% region, some slack variables $\boldsymbol{\delta} = \{\delta_{\min}, \delta_{\max}\}$ are added to the optimization problem; therefore the constraints on the glucose become $\hat{y}(j|k) \in \mathcal{Y}_{j,\delta},\ \forall j \in \mathbb{I}_1^N$, with

$$\mathcal{Y}_{j,\delta} = \left\{y : y_{\min}(j) - \delta_{\min}(j) \le y \le y_{\max}(j) + \delta_{\max}(j)\right\}, \tag{14}$$

where $y_{\min}$ and $y_{\max}$ are the extreme values of $\mathcal{Y}_j$ from (9).

3.1. Terminal ingredients computation

The tightened constraints are computed as described in the previous section, for all subjects, only once and offline. This tightening implies the definition of the length of the control horizon N_c, which may vary for each virtual patient. The control horizon is calculated as the maximum possible value that makes it possible to have a set of constraints that is not empty, but it also takes into account the need to have reasonable ranges according to the system.

A prediction horizon N_p longer than the control horizon N_c is considered to increase the domain of attraction and the predictive ability of the controller, thus $N_p > N_c$. A local control law for the predictions from N_c to N_p must be established to apply this approach. We use the following:

$$u = K(\bar{x} - x) + \bar{u}, \tag{15}$$

with $u = (u_1, u_2)$ and where $K \in \mathbb{R}^{n_u \times n_x}$ is the control gain of a Linear Quadratic Regulator (LQR) and $(\bar{x}, \bar{u})$ is an equilibrium point around which the system $\hat{F}(x, u)$ is linearized. In particular, $\bar{x}$ is constructed as per (1), using $\bar{y} = 120$ mg/dL of glucose, and $\bar{u} = (0, u_{\text{ref}})$. Matrices $A \in \mathbb{R}^{n_x \times n_x}$ and $B \in \mathbb{R}^{n_x \times n_u}$ of the linearized model $x(k+1) = Ax(k) + Bu(k)$, are calculated numerically from the input–output data using the CHoKI model. In this way, each element $A(j, i)$ and $B(j, i)$ is obtained by considering that

$$A(j,i) = \frac{\partial \hat{F}_j}{\partial x_i} = \frac{\hat{F}_j(\bar{x}_i + \epsilon) - \hat{F}_j(\bar{x}_i - \epsilon)}{2\epsilon}, \quad B(j,i) = \frac{\partial \hat{F}_j}{\partial u_i},$$

where ϵ can be different for each subject (see Table 2). Note that $A(1,1) = \frac{\partial y_{k+1}}{\partial y_k}$ and $B(1,1) = \frac{\partial y_{k+1}}{\partial u_{1,k}}$.

3.2. Insulin on board

The MPC algorithm also includes a dynamic safety constraint on the maximum basal insulin value, which is based on the amount of IOB. The IOB represents the quantity of injected insulin still active in the body, which depends on patient dynamics and on the duration of insulin action (DIA). The IOB at each sampling time k can be estimated considering the residuals of the past insulin administration, which means having:

$$IOB(k) = a(k-1)u_b(k-1) + \cdots + a(k - n_{\text{IOB}})u_b(k - n_{\text{IOB}}), \tag{16}$$

where the insulin action curve is represented by a and the vector of the insulin boluses administration history is u_b. The time of insulin action is n_{IOB}, considered with a sampling time of 5 min. Specifically, in this case, it is $n_{\text{IOB}} = 72$, which means considering 6 h (note that taking into account an insulin duration of 6 h is a less conservative approach than considering a duration of 8 h) (León-Vargas, Garelli, De Battista, & Vehí, 2013).

The upper constraint is considered to limit the basal corrections, in order to avoid giving too much insulin, and thus to reduce the risk of hypoglycemic events. This means that the basal insulin amount u_2 must be inside the new range

$$\mathcal{U}_2 = \{u : 0 \le u \le u_2^{\max}\}, \tag{17}$$

where $u_2^{\max}$ is the value of the upper constraint for the basal computation and it comes from:

$$u_2^{\max}(k,j) = \begin{cases} u_2^{\lim} - IOB(k,j) & \text{if } u_2^{\lim} > IOB(k,j) \\ u_{\text{ref}} & \text{otherwise} \end{cases} \tag{18}$$

where $u_2^{\lim} = 500$ pmol is the basal insulin maximum amount that can be injected, and considering the sampling time k and $j = 0, \ldots, N_p - 1$ (Ellingsen et al., 2009). The IOB varies along the prediction horizon (i.e. with j), which means that the estimations decrease according to the insulin action curve, without considering possible new meal boluses. This implies that the basal upper bound is equal to the reference value u_{ref} when the maximum limit $u_2^{\lim}$ is less than the insulin still active from the previous boluses injection (i.e. IOB), otherwise, the upper bound is equal to the difference between $u_2^{\lim}$ and $IOB(k)$. The weights of the insulin action curve a are obtained from $\left((DIA - t_b)/DIA\right)$, where $DIA =$ 6 h and t_b is the time passed from the previous bolus. In Fig. 2 an example of the IOB estimation for virtual Adult 10 is reported. This shows that (16) approximates quite well the real values (blue line) and the choice of DIA equal to 6 h is appropriate. The initial IOB value after a bolus could be different between the two curves. This is because the estimated IOB is based on the value of the bolus calculated for the meal, on the other hand, the real IOB is based on the value that is actually injected, which may vary from the calculated value due to pump noise.

Remark 2. To address any potential infeasibilities during the MPC resolution, N_p slack variables δ_u were included in the optimization problem. These were added to the upper bound $u_2^{\max}$ in Eq. (17), obtaining

$$\mathcal{U}_2' = \left\{u(j) : 0 \le u(j) \le u_2^{\max}(j) + \delta_u(j)\right\},\ \forall j \in \mathbb{I}_0^{N_p-1}. \tag{19}$$

3.3. CHoKI-based MPC implementation

Starting from the proposal in Sonzogni et al. (2023), the MPC optimization problem which considers also the IOB is set as follows:

$$\min_{u_2, y_a, \delta_{\text{hyper}}, \delta_{\text{hypo}}, \delta_{\min}, \delta_{\max}, \delta_u} V_N(\hat{x}, u; \Theta, \mathcal{D}) \tag{20a}$$

$$\text{s.t. } \hat{x}(0|k) = x(k) \tag{20b}$$

$$\hat{x}(j+1|k) = \hat{F}\left(\hat{x}(j|k), u_1(j), u_2(j)\right),\ j \in \mathbb{I}_0^{N_c-1} \tag{20c}$$

$$\hat{x}(j+1|k) = \hat{F}\left(\hat{x}(j|k), K(\bar{x} - x(j)) + \bar{u}\right),\ j \in \mathbb{I}_{N_c}^{N_p-1} \tag{20d}$$

$$\hat{y}(j|k) = M\hat{x}(j|k),\ j \in \mathbb{I}_0^{N_p-1} \tag{20e}$$

$$u_2(j) \in \mathcal{U}_2',\ j \in \mathbb{I}_0^{N_p-1}, \tag{20f}$$

$$\hat{y}(j|k) \in \mathcal{Y}_{j,\delta},\ j \in \mathbb{I}_0^{N_c-1} \tag{20g}$$

$$\hat{y}(j|k) \in \mathcal{Y}_{N_c,\delta},\ j \in \mathbb{I}_{N_c}^{N_p-1} \tag{20h}$$

$$u_1(j) = 0,\ j \in \mathbb{I}_1^{N_p-1} \tag{20i}$$

$$70 - \delta_{\text{hypo}} \le y_a \le 140 + \delta_{\text{hyper}} \tag{20j}$$

$$\delta_{\text{hyper}} \ge 0,\ \delta_{\text{hypo}} \ge 0 \tag{20k}$$

$$\delta_{\min}(j) \ge 0,\ \delta_{\max}(j) \ge 0,\ j \in \mathbb{I}_0^{N_p-1} \tag{20l}$$

$$\delta_u(j) \ge 0,\ j \in \mathbb{I}_0^{N_p-1} \tag{20m}$$

where (20i) is used since the meals are not predictable, $\mathcal{Y}_{j,\delta}$ comes from (14) and (20f) is the constraint that takes into consideration

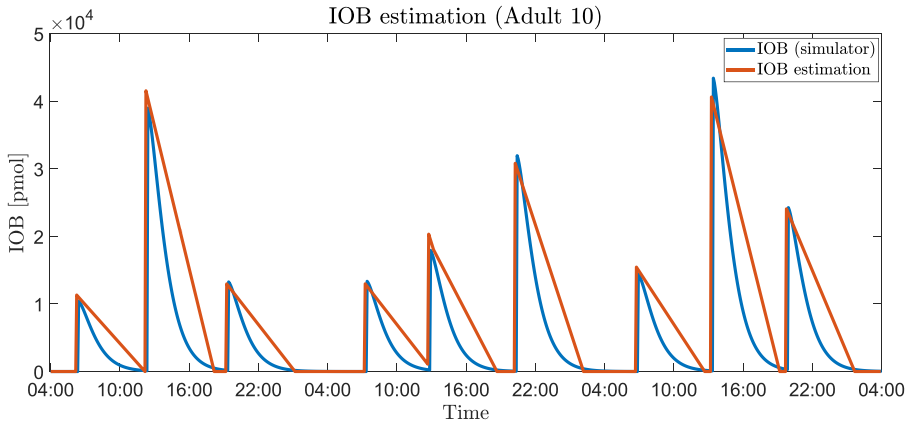

Fig. 2. The estimated boluses IOB is represented as the orange line and the IOB computed by the simulator is in blue. This is an example of the virtual patient Adult 10.

the IOB, from (19). The tightened constraints are computed as explained in the previous section, for all the subjects, and the resulting N_c are reported in Table 2. The prediction horizon is set to $N_p = 12$ for all subjects, to reach 60 min of predictions.

The cost function $V_N(\hat{x}, u; \Theta, \mathcal{D})$ to be minimized is designed by summing several components, namely:

$$V_N(\hat{x}, u; \Theta, \mathcal{D}) = V_{N_c} + V_{N_p} + V_s + \lambda V_P + V_\delta + V_u. \tag{21}$$

Specifically, the stage costs V_{N_c}, along the control horizon $N_c - 1$, and V_{N_p}, along the prediction horizon $N_p - 1$ starting from N_c, are:

$$V_{N_c} = \sum_{j=0}^{N_c-1} \|\hat{y}(j|k) - y_a\|_Q^2 + \|u_2(j) - u_{\text{ref}}\|_R^2, \tag{22a}$$

$$V_{N_p} = \sum_{j=N_c}^{N_p-1} \|\hat{y}(j|k) - y_a\|_Q^2. \tag{22b}$$

where the insulin target u_{ref} is the constant basal insulin dose delivered by the UVA/Padova simulator for the default continuous therapy of the selected virtual patient. For the implementation of the MPC in a zone control fashion is required the presence of the setpoint y_a, which is an auxiliary optimization variable and it has to be within 70 and 140 mg/dL. Two slack variables δ_{hypo} and δ_{hyper} are added to this interval for y_a, which are other optimization variables used to increase the range in the constraints when necessary. Therefore, an additional stationary cost V_s has to be considered. In V_s, the slack variables are weighted by some constants, that are set to be $p_{\text{hypo}} > p_{\text{hyper}}$ to reflect the higher danger of hypoglycemia compared to hyperglycemia (Abuin et al., 2020).

$$V_s = p_{\text{hyper}}\delta_{\text{hyper}}^2 + p_{\text{hypo}}\delta_{\text{hypo}}^2. \tag{23}$$

The terminal cost V_P penalizes the difference between the last state $\hat{x}(N_p|k)$ and the reference state (x_{ref}, which contains the set point y_a, no meals and u_{ref}).

$$V_P = \|\hat{x}(N_p|k) - x_{\text{ref}}\|_P^2, \tag{24}$$

where P is the solution to the Riccati equation, given the LQR control gain K for the linearized system around the reference point (in Section 3.1). The terminal cost is normally used to ensure the stability of the MPC and in this case, it is weighted by a factor $\lambda > 0$, as no terminal constraint is taken into account.

Other slack optimization variables are considered in the glycemic constraints (14). Thus, for the same reason as before, the cost V_δ must be included to penalize them by considering two weights, where $p_{\min} > p_{\max}$,

$$V_\delta = \sum_{j=1}^{N_P} \|\delta_{\min}(j)\|_{p_{\min}}^2 + \|\delta_{\max}(j)\|_{p_{\max}}^2. \tag{25}$$

The last component is the cost V_u, to penalize additional slack variables δ_u which are included in the control action constraints (20f),

$$V_u = \sum_{j=1}^{N_P} \|\delta_u(j)\|_{p_u}^2. \tag{26}$$

Furthermore, many combinations of weights were tested and the following were selected: $R = 10$, $p_{\text{hypo}} = 1 \cdot 10^7$, $p_{\text{hyper}} = 1 \cdot 10^6$, $p_{\min} = 1 \cdot 10^7$, $p_{\max} = 1 \cdot 10^6$, $p_u = 1 \cdot 10^7$ and $\lambda = 10$. The values of Q are shown in Table 2 and note that in the cases where R is greater than Q, this means that a more conservative controller is applied.

4. Results

The proposed MPC was tested on the virtual adult patients of the UVA/Padova simulator, with customized controllers for each subject. Three days were simulated, with the following three meals per day: 20 g at 06:00am, 90 g at 12:00pm, and 30 g at 07:00pm for the first day; 30 g at 07:00am, 80 g at 12:30pm, and 50 g at 08:00pm for the second day; and 40 g at 06:30am, 100 g at 01:00pm, and 60 g at 07:30pm for the last day. The meals were announced, and the postprandial boluses were computed by the simulator and injected 20 min after the meal's start. All the devices have the same noise setting as in the data acquisition stage, including the carbohydrate estimation error with a normal distribution with a standard deviation equal to 30% of the meal amount, for the bolus computation.

The results of the simulations for all patients are shown in Fig. 3. The top graph displays the BG trends caused by the insulin injections depicted in the bottom graph, which vary based on the patient model. The primary objective is to reduce the frequency and the severity of hypoglycemic events, which are very dangerous in the short term, and it can be seen that such a result is achieved. There are some hyperglycemic peaks, in particular for the Adult 7, who goes above 300 mg/dL, with a solution that is still feasible thanks to the slack variables in the constraints. This is due to the MPC setup which ends up being over-conservative.

The results obtained in this work are compared to the ones realized following the procedure reported in Sonzogni et al. (2023),

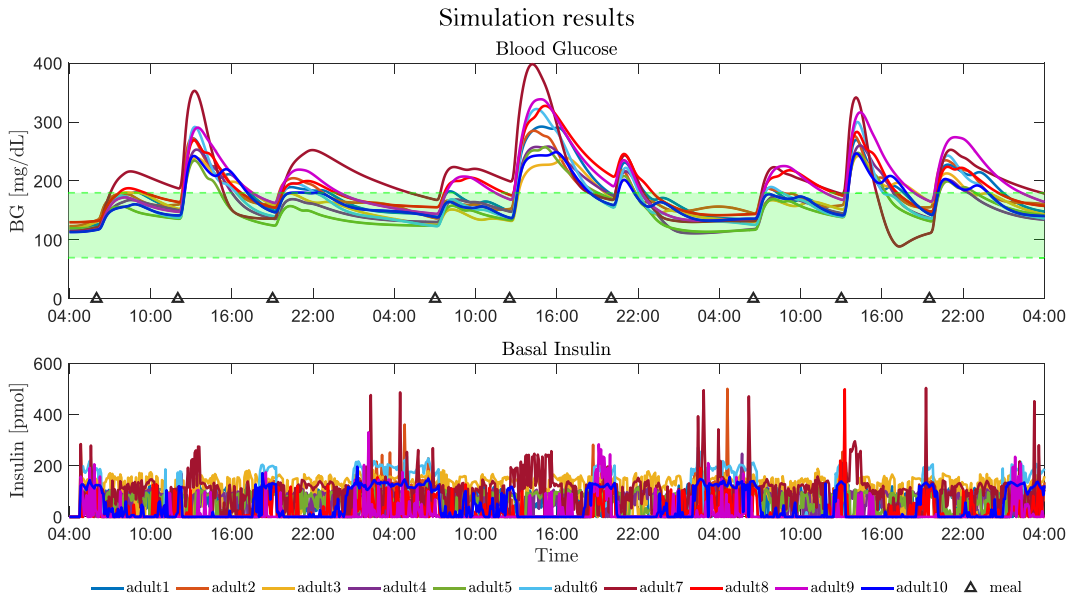

Fig. 3. The upper plot displays BG trends for all patients. The green zone represents the safe range and the black triangles depict meals. The lower plot shows basal insulin injections computed by the proposed MPC.

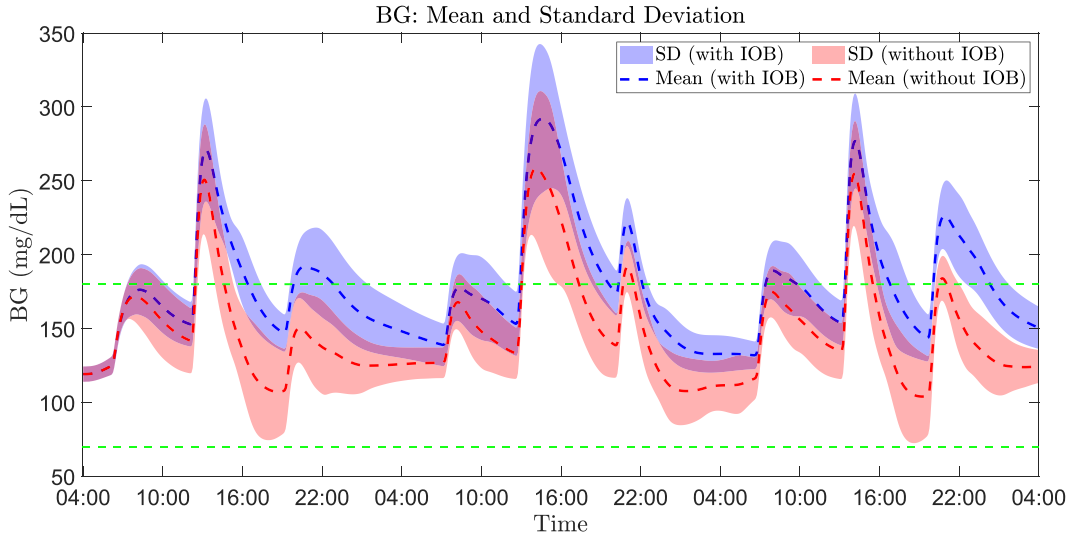

Fig. 4. Comparison of the BG values: the mean and the standard deviation of the simulations performed with IOB constraints are represented in blue, and without them are in red.

whose simulations are conducted without the IOB constraints. In particular, the comparison of the mean and standard deviation of the BG values for the two cases is shown in Fig. 4, where the blue dotted line represents the mean values of the cases with the IOB constraints and the blue area displays their standard deviations, while the cases without the IOB are in red. This indicates that including the IOB in the constraints means to have a more conservative controller, since the BG level is higher in the cases with the IOB safety constraints. It is also confirmed looking at the BG and basal insulin average values reported in Table 3 (i.e. mean and standard deviation), where the average BG values of the simulations with IOB constraints are higher than in the ones without them, because of less insulin amount. This is due to the fact that the controller does not manage post-prandial boluses. As a result, when the BG value is high at mealtime, the bolus amount tends to be higher (computed by the simulator). This leads to higher IOB, which in turn limits the basal corrections.

Another important tool for assessing AP performance is the Time In Ranges (TIRs). This shows the percentage of time a patient spends in each specific BG range. In particular, as required by the American Diabetes Association (ADA), the TIRs targets are as follows: $<$ 5% of time with BG higher than 250 mg/dL, $<$ 25% between 180-250 mg/dL, $>$ 70% between 70-180 mg/dL, $<$ 4% between 55-70 mg/dL and $<$ 1% for BG lower than 55 mg/dL. The proposed controller ensures that the requirements for the hypoglycemic ranges are always met, which is the main objective. However, the controller permits the subjects to stay a little longer in the two hyperglycemic ranges, which also means that they stay within the 70-180 mg/dL range for less than 70% of the simulation time. The results are displayed in Fig. 5, where, for each subject, the graph on the left is for the cases without the IOB, while the one on the right is for the cases with the IOB constraints.

The conservative results are a consequence of the linear function used to estimate the IOB. In fact, as shown in Fig. 2, the IOB

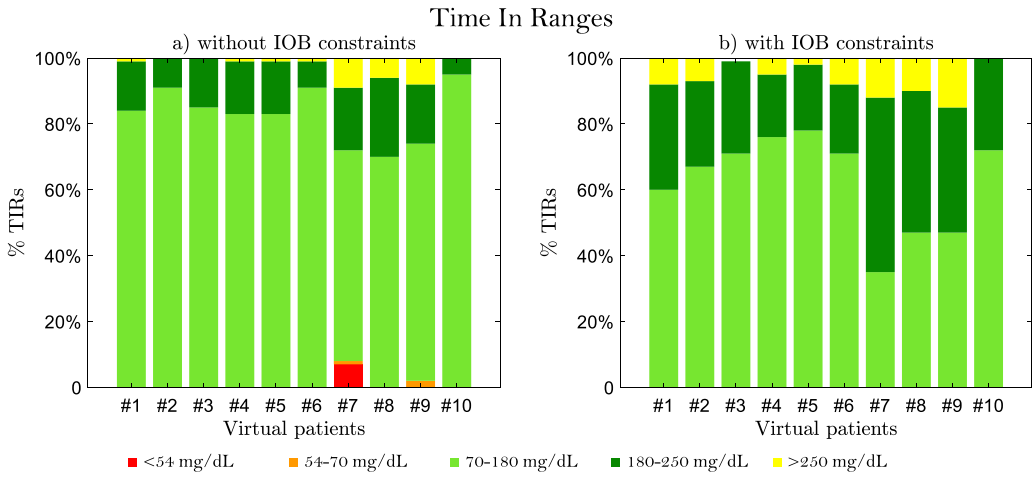

Fig. 5. TIRs results of the simulations performed with (graph on the right) and without the IOB constraints (graph on the left). Each bar represents a specific subject.

Table 3
Comparison of the BG mean and standard deviation (in mg/dL), of the basal insulin u_2 mean and standard deviation (in pmol), and GRI for the controller with (on the right) and without (on the left) the IOB constraints.

Adult	Without IOB constraint			With IOB constraint		
	BG mean ± std [mg/dL]	u_2 mean ± std [pmol]	GRI	BG mean ± std [mg/dL]	u_2 mean ± std [pmol]	GRI
#1	159.78 ± 30.27	92.71 ± 46.78	14.15	180.27 ± 38.89	68.42 ± 48.17	38.20
#2	140.16 ± 27.15	114.09 ± 55.68	7.12	178.99 ± 34.44	35.70 ± 62.60	31.72
#3	152.05 ± 27.50	133.43 ± 42.58	12.21	168.81 ± 30.65	114.00 ± 57.49	23.40
#4	154.08 ± 33.94	71.86 ± 41.67	14.61	164.28 ± 37.47	64.56 ± 39.02	23.31
#5	147.05 ± 34.62	78.31 ± 31.37	13.78	156.21 ± 34.58	68.00 ± 33.14	18.96
#6	126.17 ± 37.56	184.03 ± 39.44	7.58	171.12 ± 45.56	52.49 ± 83.82	29.87
#7	151.86 ± 70.35	102.92 ± 95.51	53.87	197.67 ± 59.71	93.18 ± 72.71	61.23
#8	169.55 ± 37.75	53.39 ± 68.33	28.95	191.58 ± 41.80	20.36 ± 40.42	50.50
#9	159.26 ± 52.18	55.32 ± 72.10	31.26	194.82 ± 50.46	13.74 ± 41.78	55.03
#10	119.26 ± 28.86	120.24 ± 25.11	4.35	168.43 ± 31.11	43.90 ± 56.27	22.75

is always overestimated. This can be improved searching for a polynomial or exponential function.

An additional useful tool can be the Glycemia Risk Index (GRI) (Klonoff et al., 2022), which is a quantitative measure designed to provide a comprehensive evaluation of an individual's susceptibility to hypoglycemia or hyperglycemia. It is obtained from

$$GRI = \Big(3.0\big(p_1 + 0.8p_2\big)\Big) + \Big(1.6\big(p_4 + 0.5p_3\big)\Big),$$

where the first part is the hypoglycemic component and the second is the hyperglycemic one. It considers the same percentages of the TIRs, where p_1 is the percentage of time in which the subject's BG is less than 54 mg/dL, p_2 for the BG between 54 and 70 mg/dL, p_3 for the BG between 180 and 250 mg/dL and p_4 for BG higher than 250 mg/dL. The GRI can be displayed graphically on a grid with the hypoglycemia component on the horizontal axis and the hyperglycemia component on the vertical axis. Diagonal lines divide the graph into five zones (quintiles) based on overall glycemia quality, from best (0^{th}-20^{th} percentile) to worst (81^{st}-100^{th} percentile).

The GRI values are reported in Table 3, while the two components are represented in Fig. 6b to understand which is the higher one, where each dot on the graph describes a specific subject in the cases without the IOB, and the squares are for the ones with the IOB constraints. In the cases without the IOB, Adult 7 is in Zone C, Adult 8 and Adult 9 are in Zone B, and the others are in safe Zone A. While in the cases with IOB, due to the higher BG values, Adult 7 is in Zone D, Adult 8 and Adult 9 are in Zone C, Adult 5 in Zone A and the others are in Zone B. All the subjects (except for Adult 7 and Adult 9 in the cases without the IOB constraint, due to the hypoglycemic events highlighted in Fig. 5a) lay on the y-axis, this is because our controller is designed to avoid hypoglycemia, which is why the higher risk component is the hyperglycemic one.

Up to now, the average results are evaluated, but to have a more complete analysis, also the Control-Variability Grid Analysis (CVGA) can be assessed. The CVGA (Magni et al., 2008) is a graphical representation that provides both visual and numerical information about the quality of glycemic control. In Fig. 6a, each dot on the graph describes a specific subject in the cases without IOB, while the squares are for those with IOB restrictions, with the minimum BG value as the x-coordinate and the maximum BG value as the y-coordinate. As recommended by Magni et al. (2008), the lower bound of CVGA is set at 2.5% of the distribution of data and the upper bound at 97.5%. Considering the simulations with the IOB, these worst cases are all in the safe zones (except for Adult 7, Adult 8 and Adult 9, who are in Zone C). This demonstrates how including the IOB constraint resolves the issues related to hypoglycemic events, increasing the minimum BG value, even at the cost of also increasing the maximum value, thus moving the squares up vertically on the graph.

The current controller may be too conservative, especially for Adult 7, as it keeps the virtual patient in a hyperglycemic state for an extended period. Consequently, further analysis is necessary to improve control, especially considering the patient's high variability and complex response to insulin.

4.1. Simulations with insulin sensitivity variations

In this Section, the proposed CHoKI-based MPC with the IOB constraints is tested on the same virtual patients, but with variations in the insulin sensitivity, thanks to the availability of

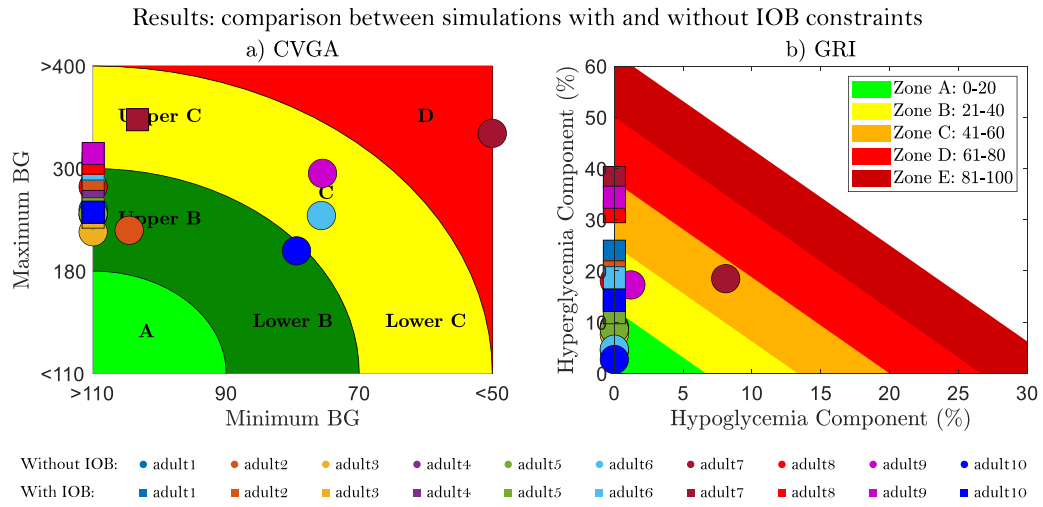

Fig. 6. Results of the simulations performed with the IOB constraints (squares), compared to the ones without them (dots): a) CVGA and b) GRI.

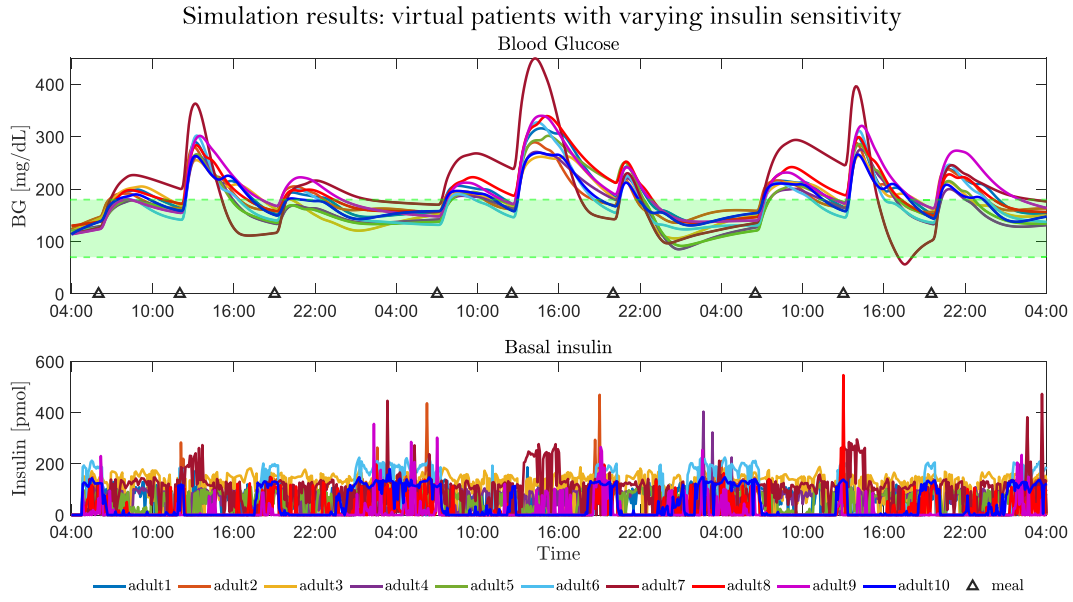

Fig. 7. Proposed controller applied to the virtual patients with varying insulin sensitivity. Upper plot: BG trends of all patients, with the green zone for the safe range and the black triangles for the meal times. Lower plot: basal insulin injections.

the circadian variability option in the updated version of the UVA/Padova simulator (DMMS.R version 1.3). Insulin sensitivity refers to how responsive the cells are to insulin and this can vary in the subject during the day (Visentin, Dalla Man, Kudva, Basu, & Cobelli, 2015). The simulations are performed with the same setting as in the previous cases and the results are presented in Fig. 7, where the upper part shows the BG trends that are obtained thanks to the insulin injections displayed in the lower graph. To better evaluate the performances of the proposed controller in managing the variations in the insulin sensitivity, the CVGA, GRI and TIRs results are considered as well (see Fig. 8a, Fig. 8b and Fig. 9, respectively).

The cases reported in this Section derive from the attempt to control a more complex system due to the variability of insulin sensitivity, which affects the relationship between glucose, insulin, and carbohydrates. This leads to more fluctuations in glucose levels, as depicted in the upper part of Fig. 7. This is evident when looking at Adult 7, who worsens compared to the case without variability (as shown in Fig. 3), both because the hyperglycemia peak is higher, but also due to greater fluctuations in glucose level, since the patient goes also in hypoglycemia (but $>$ 54 mg/dL). Fig. 8a shows the CVGA outcomes, where Adult 7 is in the D zone, Adult 5, 6 and 9 are in the Upper C zone, while the others are in the Upper B zone. Fig. 8b displays the GRI values, where Adult 7 is in Zone D, while Adult 4, 5 and 6 are in Zone B, and the remaining ones are in Zone C. These results are quite promising, since they demonstrate that the proposed controller can still prevent hypoglycemic events while remaining conservative, even in the presence of insulin variability. However, the variations in insulin sensitivity affect the ability of the CHoKI learning method, even if the outcomes are similar to the previous case, leading to hyperglycemic events (see Adult 7).

The CHoKI technique estimates the parameters $\mathcal{L}$ and $\mathcal{P}$ once and offline. To better manage the insulin variability a possible solution could be to use an adaptive CHoKI, which can update $\mathcal{L}$ and $\mathcal{P}$ values depending on the blood glucose and insulin situation.

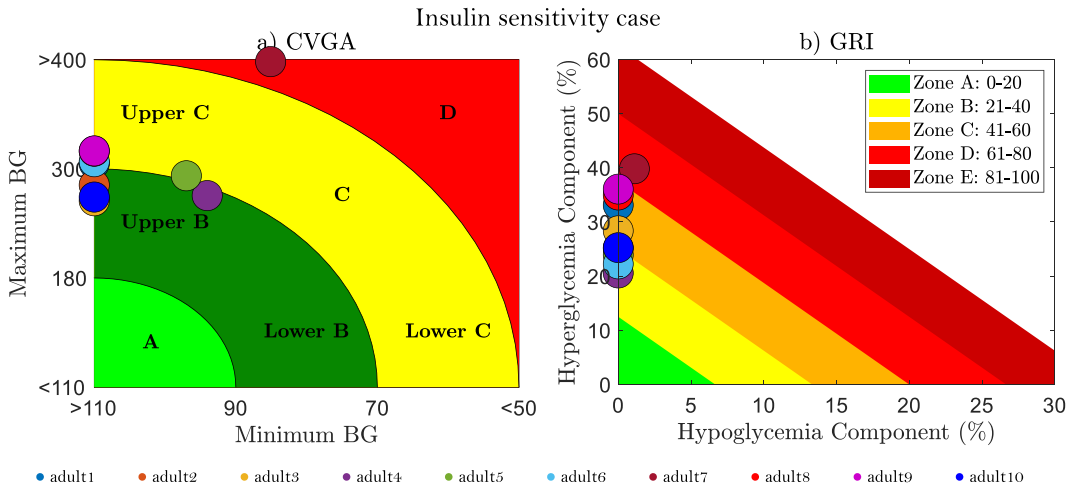

Fig. 8. Results of the simulations performed with the IOB constraints, applied to the varying insulin sensitivity case: a) CVGA and b) GRI.

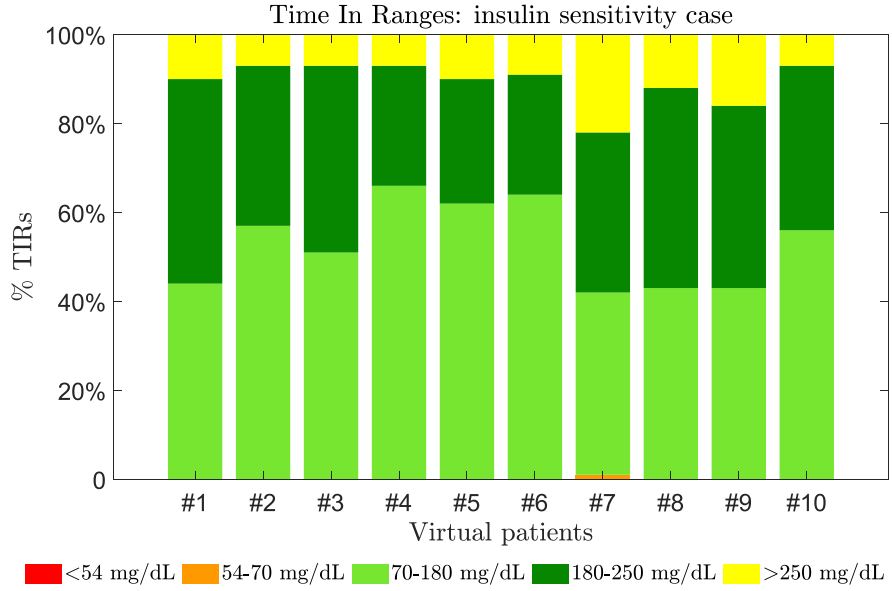

Fig. 9. TIRs results of the simulations performed with the IOB constraints, applied to the varying insulin sensitivity case.

4.2. Simulations with insulin sensitivity variations and physical activity

Physical Activity (PA) has many benefits for T1D patients, including enhancements in cardiorespiratory fitness, in the body composition, in achieving the glycemic goals, and in the overall quality of life (American Diabetes Association, 2004; Riddell et al., 2017). On the other hand, there are many factors that affect the relationship between insulin and glucose levels, which can thus create issues for the patient, primarily due to the risk of hypoglycemia.

This is why, in this Section, the PA is included in the analysis. The simulations are set up in the same way as described in Section 4.1, adding also training sessions. PA is not announced, it is considered as an external disturbance, and it is involved so to analyze its impact on glucose, verifying the performance of the proposed controller in managing these variations.

Specifically, the UVA/Padova allows to add PA by setting the starting time, the duration, and the intensity level (expressed as a percentage of the oxygen consumption maximum rate, $\%VO_2^{max}$). In this work, PA was performed, at different times, on the first and third day of the simulation. This is done to alternate between a day of exercise and a day of rest, avoiding more than two days without PA, as recommended by the ADA (Colberg et al., 2016). To reproduce a physical activity session, including warm-up, high-intensity resistance bursts, aerobic exercise, and cool-down phases, the following plan is implemented: light intensity for 10 min (25% VO_2^{max}), high intensity for 10 min (65% VO_2^{max}), moderate intensity for 20 min (50% VO_2^{max}), and light intensity for 5 min (25% VO_2^{max}) (Licini et al., 2024).

The results are reported in Fig. 10, where in the lower graph there are the basal insulin injections, while in the upper graph there are the BG values, the meals (i.e. the black triangles) and the PA, represented as horizontal lines with different colors according to the intensity level. Fig. 11a shows the CVGA outcomes, while Fig. 11b shows the GRI results. Adding PA introduces more variability in the scenario, leading to increased BG oscillation. This is particularly evident in Adult 7, which goes both in hyper- and hypoglycemia ranges. In fact, the CVGA point is in the C zone, especially due to hyperglycemic issues (visible in the TIRs in Fig. 12), this is confirmed also by looking at the GRI, which is equal to 64.28, thus in the D zone. The controller is able to

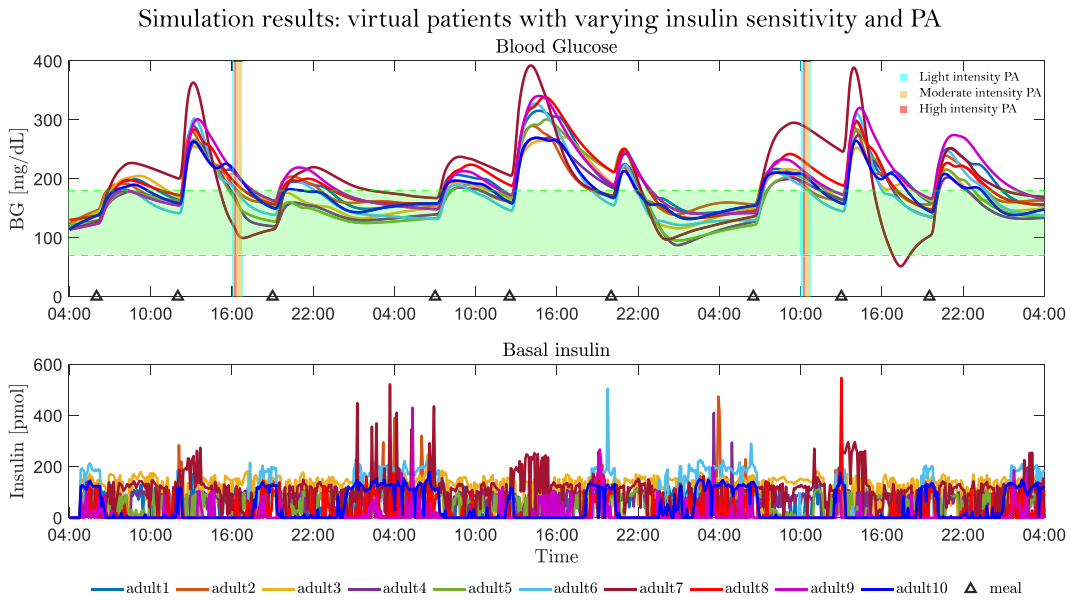

Fig. 10. Proposed controller applied to the virtual patients with varying insulin sensitivity and PA. Upper plot: BG trends of all patients, with the green zone for the safe range and the black triangles for the meal times. The horizontal lines depict the PA, considering light blue for the light intensity, yellow for the moderate intensity, and red for the high intensity PA. Lower plot: basal insulin injections.

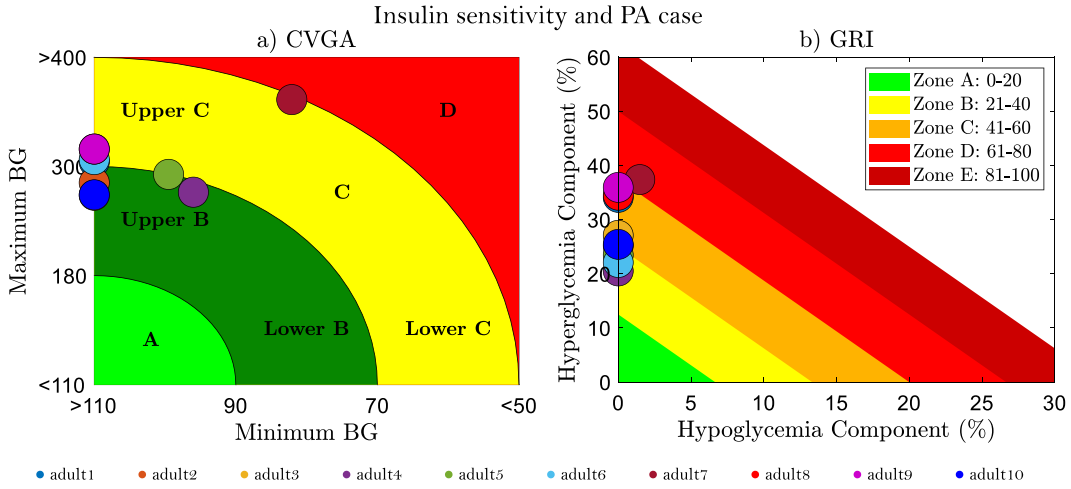

Fig. 11. Results of the simulations performed with the IOB constraints, applied to the varying insulin sensitivity case with PA: a) CVGA and b) GRI.

manage also this disturbance, since the outcomes are similar to the previous cases, being conservative. This can be seen in Fig. 12, where the TIRs results show that all the virtual patients stay in hyperglycemic ranges for high percentages of the time and never in hypoglycemia (except for Adult 7).

There exist some guidelines for hypoglycemia prevention, based on carbohydrate requirements and glucose concentration before exercise (Riddell et al., 2017). These suggestions to the patient include consuming carbohydrates before or during physical activity, delaying the session if BG is too low, and continuously monitoring glycemia.

Remark 3. The outcomes and performances reported in this Section are *in silico* results, since they are obtained by applying the proposed control algorithm to the virtual adult patients of the UVA/Padova simulator. This means that such results may differ from those that might be obtained if the proposal was applied to a real patient.

5. Conclusion

A new MPC algorithm based on the CHoKI learning method was proposed to be used in the AP for managing basal insulin in T1D patients, including IOB estimation to limit the amount of basal insulin injections. The whole system was tested on the virtual patients of the UVA/Padova simulator. The proposed controller aims to drive and maintain the BG level inside the euglycemic range most of the time, trying to avoid the more dangerous hypoglycemic events. The obtained results seem promising, since the estimation of the IOB in the MPC helps in achieving such an aim. To decrease the level of the hyperglycemic events, the IOB estimation could be improved. In particular, a polynomial or exponential curve can be tried instead of the linear weights employed in this case.

The outcomes end up being conservative, however this conservativeness is a limitation of the CHoKI learning method (Manzano et al., 2021). Therefore, future work will focus on finding new methods to reduce this limitation.

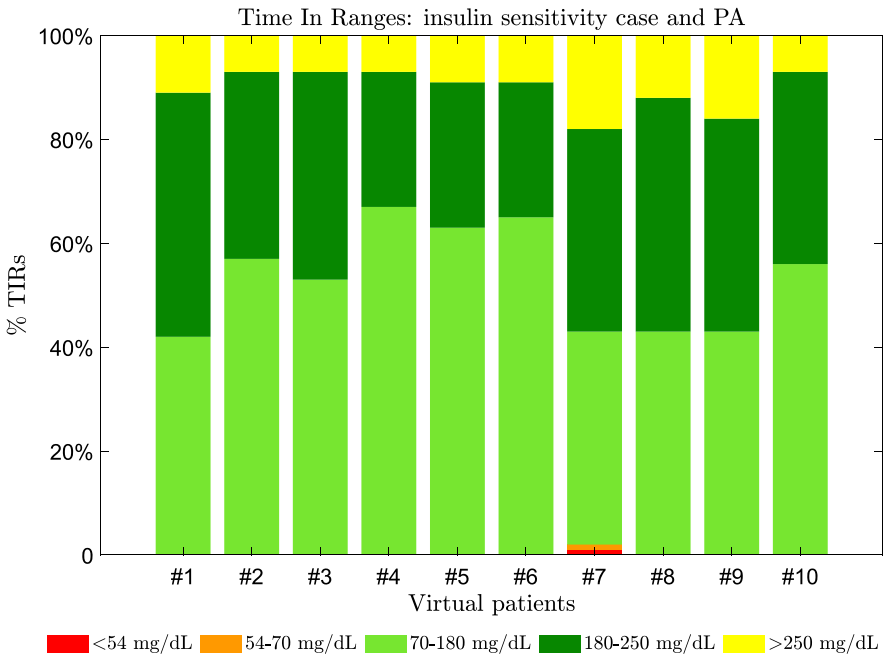

Fig. 12. TIRs results of the simulations performed with the IOB constraints, applied to the varying insulin sensitivity case, with PA.

The proposed controller was also tested on virtual patients with variability in insulin sensitivity and also considering physical activity, to evaluate the performances of the proposal under more challenging scenarios. To improve these results, the next step for future works could be to identify multi-models, dividing the day into some intervals (such as breakfast, lunch and dinner) and trying to learn different behavior, with the aim of controlling patients more accurately, thanks to the inclusion of the analysis of insulin sensitivity variations during the day.

CRediT authorship contribution statement

Beatrice Sonzogni: Writing – review & editing, Writing – original draft, Validation, Investigation, Formal analysis, Conceptualization. **José María Manzano:** Supervision, Formal analysis, Conceptualization. **Marco Polver:** Investigation, Formal analysis. **Fabio Previdi:** Supervision, Funding acquisition. **Antonio Ferramosca:** Supervision, Formal analysis, Conceptualization.

Declaration of competing interest

The authors declare that they have no known competing financial interests or personal relationships that could have appeared to influence the work reported in this paper.

Acknowledgments

This work was funded by the National Plan for NRRP Complementary Investments (PNC, established with the decree-law 6 May 2021, n. 59, converted by law n. 101 of 2021) in the call for the funding of research initiatives for technologies and innovative trajectories in the health and care sectors (Directorial Decree n. 931 of 06-06-2022) - project n. PNC0000003 - AdvaNced Technologies for Human-centrEd Medicine (project acronym: ANTHEM). This work reflects only the authors' views and opinions, neither the Ministry for University and Research nor the European Commission can be considered responsible for them.

Data availability

The data that has been used is confidential.

References

Abuin, Pablo, Rivadeneira, Pablo S., Ferramosca, Antonio, & González, Alejandro Hernán (2020). Artificial pancreas under stable pulsatile MPC: Improving the closed-loop performance. *Journal of Process Control*, *92*, 246–260.

American Diabetes Association (2004). Physical activity/exercise and diabetes. *Diabetes Care*, *27*(suppl_1), s58–s62.

Cairoli, Francesca, Fenu, Gianfranco, Pellegrino, Felice Andrea, & Salvato, Erica (2020). Model predictive control of glucose concentration based on signal temporal logic specifications with unknown-meals occurrence. *Cybernetics and Systems*, *51*(4), 426–441.

Colberg, Sheri R., Sigal, Ronald J., Yardley, Jane E., Riddell, Michael C., Dunstan, David W., Dempsey, Paddy C., et al. (2016). Physical activity/exercise and diabetes: a position statement of the American Diabetes Association. *Diabetes Care*, *39*(11), 2065.

Del Favero, Simone, Toffanin, Chiara, Magni, Lalo, & Cobelli, Claudio (2019). Deployment of modular MPC for type 1 diabetes control: the Italian experience 2008–2016. In *The artificial pancreas* (pp. 153–182). Elsevier.

Ellingsen, Christian, Dassau, Eyal, Zisser, Howard, Grosman, Benyamin, Percival, Matthew W., Jovanovič, Lois, et al. (2009). Safety constraints in an artificial pancreatic β cell: an implementation of model predictive control with insulin on board. *Journal of Diabetes Science and Technology*, *3*(3), 536–544.

Gondhalekar, Ravi, Dassau, Eyal, & Doyle III, Francis J. (2016). Periodic zone-MPC with asymmetric costs for outpatient-ready safety of an artificial pancreas to treat type 1 diabetes. *Automatica*, *71*, 237–246.

González, Alejandro H., Rivadeneira, Pablo S., Ferramosca, Antonio, Magdelaine, Nicolas, & Moog, Claude H. (2017). Impulsive Zone MPC for Type I Diabetic Patients based on a long-term model. *IFAC-PapersOnLine*, *50*(1), 14729–14734.

González, Alejandro H., Rivadeneira, Pablo S., Ferramosca, Antonio, Magdelaine, Nicolas, & Moog, Claude H. (2020). Stable impulsive zone model predictive control for type 1 diabetic patients based on a long-term model. *Optimal Control Applications & Methods*, *41*(6), 2115–2136.

Hajizadeh, Iman, Rashid, Mudassir, & Cinar, Ali (2019). Plasma-insulin-cognizant adaptive model predictive control for artificial pancreas systems. *Journal of Process Control*, *77*, 97–113.

Hewing, Lukas, Wabersich, Kim P., Menner, Marcel, & Zeilinger, Melanie N. (2020). Learning-based model predictive control: Toward safe learning in control. *Annual Review of Control, Robotics, and Autonomous Systems*, *3*, 269–296.

Hovorka, Roman, Canonico, Valentina, Chassin, Ludovic J., Haueter, Ulrich, Massi-Benedetti, Massimo, Federici, Marco Orsini, et al. (2004). Nonlinear model predictive control of glucose concentration in subjects with type 1 diabetes. *Physiological Measurement*, *25*(4), 905.

Katsarou, Anastasia, Gudbjörnsdottir, Soffia, Rawshani, Araz, Dabelea, Dana, Bonifacio, Ezio, Anderson, Barbara J., et al. (2017). Type 1 diabetes mellitus. *Nature Reviews Disease Primers*, *3*(1).

Klonoff, David C., Wang, Jing, Rodbard, David, Kohn, Michael A., Li, Chengdong, Liepmann, Dorian, et al. (2022). A glycemia risk index (GRI) of hypoglycemia and hyperglycemia for continuous glucose monitoring validated by clinician ratings. *Journal of Diabetes Science and Technology*, 19322968221085273.

León-Vargas, Fabian, Garelli, Fabricio, De Battista, Hernán, & Vehí, Josep (2013). Postprandial blood glucose control using a hybrid adaptive PD controller with insulin-on-board limitation. *Biomedical Signal Processing and Control*, *8*(6), 724–732.

Licini, Nicola, Sonzogni, Beatrice, Abuin, Pablo, Previdi, Fabio, Gonzalez, Alejandro H., & Ferramosca, Antonio (2024). Artificial pancreas under stable pulsatile model predictive control: including the physical activity effect. In *Accepted for publication in the 63rd IEEE conference on decision and control*.

Magni, Lalo, Raimondo, Davide M., Man, Chiara Dalla, Breton, Marc, Patek, Stephen, De Nicolao, Giuseppe, et al. (2008). Evaluating the efficacy of closed-loop glucose regulation via control-variability grid analysis. *Journal of Diabetes Science and Technology*, *2*(4), 630–635.

Manzano, José María, Limon, Daniel, Muñoz de la Peña, David, & Calliess, Jan-Peter (2020). Robust learning-based MPC for nonlinear constrained systems. *Automatica*, *117*.

Manzano, José María, Muñoz de la Peña, David, Calliess, Jan-Peter, & Limon, Daniel (2021). Componentwise Hölder inference for robust learning-based MPC. *Institute of Electrical and Electronics Engineers. Transactions on Automatic Control*, *66*(11), 5577–5583.

Moon, Sun Joon, Jung, Inha, & Park, Cheol-Young (2021). Current advances of artificial pancreas systems: a comprehensive review of the clinical evidence. *Diabetes & Metabolism Journal*, *45*(6), 813–839.

Rawlings, Blake, James, & Mayne, David Q. (2009). *Model predictive control: Theory and design*. Nob Hill Pub..

Riddell, Michael C., Gallen, Ian W., Smart, Carmel E., Taplin, Craig E., Adolfsson, Peter, Lumb, Alistair N., et al. (2017). Exercise management in type 1 diabetes: a consensus statement. *The Lancet Diabetes & Endocrinology*, *5*(5), 377–390.

Shi, Dawei, Dassau, Eyal, & Doyle, Francis J. (2018). Adaptive zone model predictive control of artificial pancreas based on glucose-and velocity-dependent control penalties. *IEEE Transactions on Biomedical Engineering*, *66*(4), 1045–1054.

Sonzogni, Beatrice, Manzano, José María, Polver, Marco, Previdi, Fabio, & Ferramosca, Antonio (2023). CHoKI-based MPC for blood glucose regulation in artificial pancreas. In *Proceedings of 22nd IFAC world congress*.

Soru, Paola, De Nicolao, Giuseppe, Toffanin, Chiara, Dalla Man, Chiara, Cobelli, Claudio, Magni, Lalo, et al. (2012). MPC based artificial pancreas: strategies for individualization and meal compensation. *Annual Reviews in Control*, *36*(1), 118–128.

The Epsilon Group (2016). DMMS.R (Version 1.1) [Software]. Retrieved from https://tegvirginia.com/.

Toffanin, Chiara, Messori, Mirko, Di Palma, Federico, De Nicolao, Giuseppe, Cobelli, Claudio, & Magni, Lalo (2013). Artificial pancreas: model predictive control design from clinical experience. *Journal of Diabetes Science and Technology*, *7*(6), 1470–1483.

Visentin, Roberto, Dalla Man, Chiara, Kudva, Yogish C., Basu, Ananda, & Cobelli, Claudio (2015). Circadian variability of insulin sensitivity: physiological input for in silico artificial pancreas. *Diabetes Technology & Therapeutics*, *17*(1), 1–7.